Hindawi
Journal of Chemistry
Volume 2018, Article ID 3109047, 9 pages
https://doi.org/10.1155/2018/3109047

Research Article

Dissolution and Solubility Product of Cd-Fluorapatite [$Cd_5(PO_4)_3F$] at pH of 2–9 and 25–45°C

Ju Lin,[1] Zongqiang Zhu,[2] Yinian Zhu,[1] Huili Liu,[1] Lihao Zhang,[2] and Zhangnan Jiang[1]

[1]*College of Environmental Science and Engineering, Guilin University of Technology, Guilin 541004, China*
[2]*Guangxi Key Laboratory of Environmental Pollution Control Theory and Technology, Guilin University of Technology, Guilin 541004, China*

Correspondence should be addressed to Yinian Zhu; zhuyinian@glut.edu.cn

Received 16 April 2018; Accepted 30 July 2018; Published 30 August 2018

Academic Editor: Henryk Kozlowski

Dissolution of the synthetic cadmium fluorapatite [$Cd_5(PO_4)_3F$] at 25°C, 35°C, and 45°C was experimentally examined in HNO_3 solution, pure water, and NaOH solution. The characterization results confirmed that the cadmium fluorapatite nanorods used in the experiments showed no obvious variation after dissolution. During the dissolution of $Cd_5(PO_4)_3F$ in HNO_3 solution (pH = 2) at 25°C, the fluoride, phosphate, and cadmium ions were rapidly released from solid to solution, and their aqueous concentrations had reached the highest values after dissolution for <1 h, 1440 h, and 2880 h, respectively. After that, the total dissolution rates declined slowly though the solution Cd/P molar ratios increased incessantly from 1.55~1.67 to 3.18~3.22. The solubility product for $Cd_5(PO_4)_3F$ (K_{sp}) was determined to be $10^{-60.03}$ ($10^{-59.74}$~$10^{60.46}$) at 25°C, $10^{-60.38}$ ($10^{-60.32}$~$10^{60.48}$) at 35°C, and $10^{-60.45}$ ($10^{-60.33}$~$10^{60.63}$) at 45°C. Based on the log K_{sp} values obtained at an initial pH of 2 and 25°C, the Gibbs free energy of formation for $Cd_5(PO_4)_3F$ (ΔG_f^0) was calculated to be −4065.76 kJ/mol (−4064.11~4068.23 kJ/mol). The thermodynamic parameters for the dissolution process were computed to be 342515.78 J/K·mol, −85088.80 J/mol, −1434.91 J/K·mol, and 2339.50 J/K·mol for ΔG^0, ΔH^0, ΔS^0, and $\Delta C_p{}^0$, correspondingly.

1. Introduction

Apatite [$Ca_5(PO_4)_3(F,OH)$] forms a large family of minerals due to many isomorphous substitutions, which play a very important role in numerous industrial, medical, and environmental processes [1–3]. Apatite minerals are the raw materials to produce phosphatic fertilizers and usually contain many harmful minor elements. Among them, cadmium is one of the most toxic heavy elements in natural environment and can cause animal osteoporosis and osteomalacia due to its possible concentration in mammal's hard tissues through food chains [4–6]. Cd^{2+} (0.095 nm radius) and F^- have the probability of substitution for Ca^{2+} (0.100 nm radius) and OH^- in the vertebral animals' bones and teeth that are principally composed of calcium hydroxyapatite. Additionally, the ion exchangeability of apatite offers a possibility for the remediation of heavy metal-contaminated soils and the removal of hazardous heavy metals from industrial wastewaters. Apatite minerals have been applied to stabilize many heavy metals including cadmium [7–10].

The substitution of Cd^{2+} for Ca^{2+} in the apatite results in the formation of its isomorph, cadmium fluorapatite (Cd-FAP) [11]. Therefore, it is essential to understand its fundamental physicochemical properties, predominantly the solubility of cadmium apatite and its dissolution mechanism. Although many experimental works on the dissolution mechanism and kinetics of apatites in aqueous solution had already been executed [7, 12–16], much of them only concentrated on calcium hydroxyapatite and fluorapatite. Unfortunately, the thermodynamic data and dissolution kinetics for cadmium fluorapatite in aqueous solution under different conditions are now deficient, even though its dissolution and following release of cadmium, phosphate, and fluoride ions into water play an important role in cycling of these components.

No researches have been done on the dissolution and solubility of cadmium fluorapatite [Cd-FAP, $Cd_5(PO_4)_3F$], for which no thermodynamic data could be obtained in literatures to evaluate the environmental risk of Cd in relation with fluorapatite. In the present work, cadmium fluorapatite was synthesized by the precipitation method and characterized with different instruments. The dissolution mechanism of the synthetic cadmium fluorapatite was examined at different initial pHs and temperatures. As comparison, a similar test was also performed using the pure synthetic calcium fluorapatite (Ca-FAP). Furthermore, the aqueous concentrations of cadmium, calcium, phosphate, and fluoride ions from the experiment were used to estimate the solubility products and Gibbs free energies of formation.

2. Experimental Methods

2.1. Solid Preparation and Characterization

2.1.1. Solid Preparation. The pure cadmium fluorapatite [Cd-FAP, $Cd_5(PO_4)_3F$] was synthesized in the similar method as that used in our previous research [11]. The synthetic detail for the Cd-FAP preparation was dependent on the following precipitation: $5Cd^{2+} + 3PO_4^{3-} + F^- = Cd_5(PO_4)_3F$. In an 1 L polypropylene bottle, cadmium nitrate [$Cd(NO_3)_2{\cdot}4H_2O$] was firstly dissolved in ultrapure water to prepare 0.5 L of 0.2 mol/L Cd^{2+} solution. 0.1 L of 0.2 mol/L NaF solution and 0.3 L of 0.2 mol/L $(NH_4)_2HPO_4$ solution were then rapidly mixed with the cadmium solution in the bottle to form white suspension. The pH of the resulting mixed solution with a Cd : P : F molar ratio of 5 : 3 : 1 was adjusted to 9.00 by using NH_4OH solution, which was then stirred for 10 min at room temperature and aged at 100°C for 48 h. Finally, the white solid of cadmium fluorapatite obtained was carefully washed using ultrapure water and dried at 70°C for 48 h.

2.1.2. Characterization. A quantity of 0.01 g of the synthetic cadmium fluorapatite (Cd-FAP) was dissolved in 0.025 L of 1 M HNO_3 solution and diluted to 0.1 L in a volumetric flask with ultrapure water. The total cadmium, phosphor, and fluor contents were analyzed by a PerkinElmer inductively coupled plasma optical emission spectrometer (ICP-OES, Optima 7000DV) or a Dionex ion chromatography system (IC, ICS-2100). An X'Pert PRO diffractometer with Cu Kα radiation (40 kV and 40 mA) was applied to record the powder X-ray diffraction (XRD) pattern of Cd-FAP. Owing to no ICDD reference code for cadmium fluorapatite exist, the mineral phase was identified by comparing with the ICDD reference code for cadmium hydroxyapatite (00-014-0302). The obtained Cd-FAP nanorods were morphologically observed using a Hitachi field emission scanning electron microscope (FE-SEM, S-4800) and characterized using a Nicolet Nexus Fourier transform infrared spectrophotometer (FT-IR, 470) in a KBr pellet within 4000–400 cm^{-1}.

2.2. Dissolution Experiments. The synthetic Cd-FAP solid (2 g) was put in a series of 0.1 L bottles which were then added with 0.1 L of HNO_3 solution (pH = 2), ultrapure water (pH = 5.6), or NaOH solution (pH = 9). The capped bottles were placed in three temperature-controlled water baths (25°C, 35°C, and 45°C). The aqueous solution (5 mL) was sampled from each bottle for 20 times (1 h, 3 h, 6 h, 12 h, 24 h, 48 h, 72 h, 480 h, 720 h, 1080 h, 1440 h, 1800 h, 2160 h, 2880 h, 3600 h, 4320 h, 5040 h, 5760 h, 6480 h, and 7200 h). After each sampling, 5 mL of the corresponding initial solution was added to hold a constant solid/solution ratio. All solution samples were filtered through a 0.22 μm membrane filter and then stabilized in a 25 mL volumetric flask using 0.2% HNO_3 solution. The total cadmium, phosphor, and fluor contents were analyzed by a Dionex IC system (ICS-2100) and a PerkinElmer ICP-OES instrument (Optima 7000DV). After 7200 h dissolution, the Cd-FAP solids were taken out, rinsed with ultrapure water, dried, and analyzed with different instruments as described above.

2.3. Thermodynamic Calculations. All calculations were executed by the computer program PHREEQC using the minteq.v4.dat database (Version 3.1.2) [17]. The PHREEQC input files use order-independent keyword data blocks and are of free-format, which ease the model constructing to simulate numerous aqueous-based scenarios. The aqueous Cd^{2+}, PO_4^{3-}, and F^- activities were first computed using PHREEQC, and then, the ion activity product (IAP) for cadmium fluorapatite [$Cd_5(PO_4)_3F$] was calculated after the mass-action expression. The aqueous species Cd^{2+}, $CdOH^+$, $Cd(OH)_2^0$, $Cd(OH)_3^-$, $Cd(OH)_4^{2-}$, Cd_2OH^{3+}, CdF^+, and CdF_2^0 were included in the calculation for the total cadmium, PO_4^{3-}, HPO_4^{2-}, $H_2PO_4^-$, $H_3PO_4^0$, and $NaHPO_4^-$ for the total phosphate, and F^-, HF^0, HF_2^-, H_2F_2, NaF, CdF^+, and CdF_2^0 for the total fluoride.

3. Results and Discussion

3.1. Solid Characterization. The component of the synthesized cadmium fluorapatite [Cd-FAP, $Cd_5(PO_4)_3F$] is dependent on the initial Cd : P : F ratio molar ratio in the precursor solution. The crystal nanorods were confirmed to be the aimed composition of $Cd_5(PO_4)_3F$. The atomic Cd : P : F ratio was 5 : 3 : 1 that is the stoichiometric ratio of $Cd_5(PO_4)_3F$. No other components were detected in the white solid precipitate.

The Cd-FAP nanorods before and after dissolution were characterized using XRD, FT-IR, and FE-SEM. As showed in Figures 1–3, the synthetic Cd-FAP solids before and after dissolution were not distinguishable. No secondary minerals were evidenced after dissolution. The XRD patterns of the prepared solids are presented in Figure 1. The X-ray diffraction showed that all the solid samples were pure apatite with crystallizing in the hexagonal system $P6_3/m$, which was confirmed by comparing with the JCPDS reference for cadmium hydroxyapatite (00-014-0302) (Figure 1). The Cd-FAP solids were highly crystallized and showed the formation of apatite nanorods with the lattice parameters of $a = 9.3284$ and $c = 6.6378$.

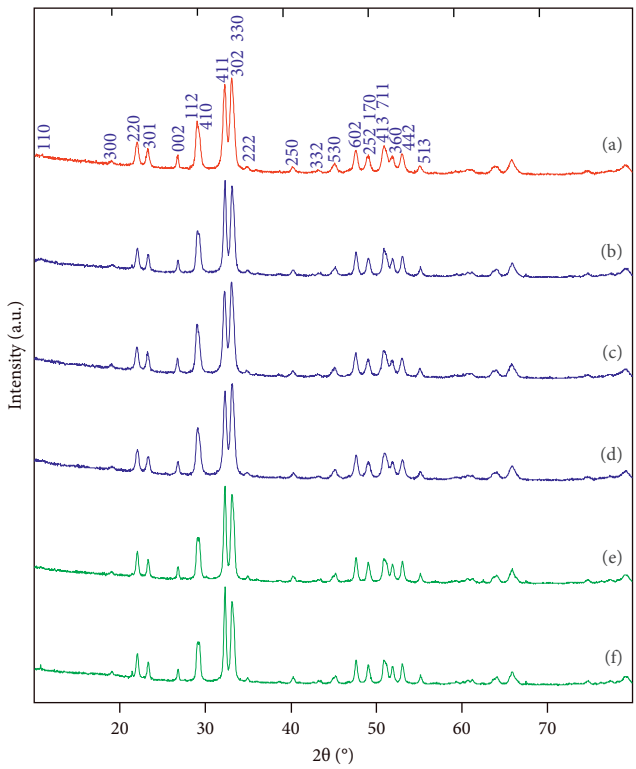

Figure 1: XRD analysis of the synthetic cadmium fluorapatite [$Cd_5(PO_4)_3F$] before (a) and after (b)–(f) dissolution at 25–45°C for 7200 h. (a) Synthetic Cd-FAP; (b) 25°C and pH = 2; (c) 25°C and pH = 5.6; (d) 25°C and pH = 9; (e) 35°C and pH = 2; (f) 45°C and pH = 2.

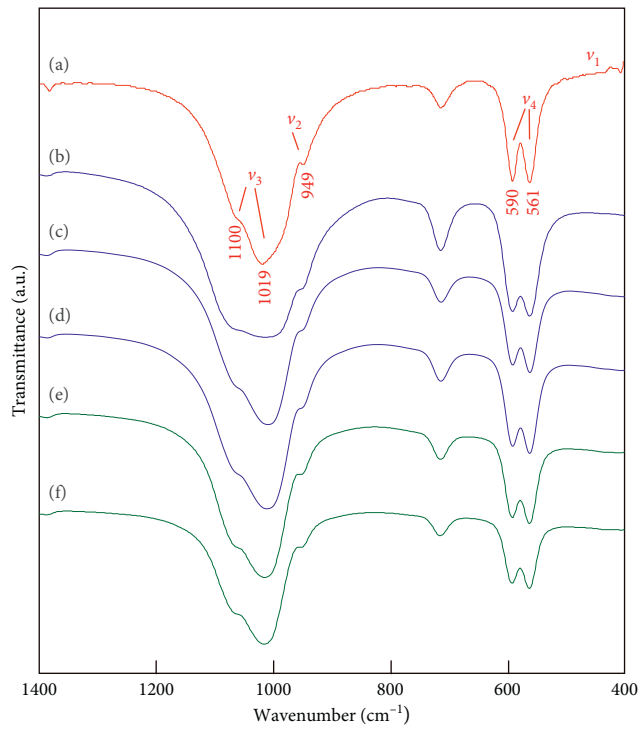

Figure 2: FT-IR analysis of the synthetic cadmium fluorapatite [$Cd_5(PO_4)_3F$] before (a) and after (b)–(f) dissolution at 25–45°C for 7200 h. (a) Synthetic Cd-FAP; (b) 25°C and pH = 2; (c) 25°C and pH = 5.6; (d) 25°C and pH = 9; (e) 35°C and pH = 2; (f) 45°C and pH = 2.

The regular mode of the tetrahedral PO_4^{3-} ions includes ν_4 (the O-P-O bending), ν_3 (the P-O stretching), ν_2 (the O-P-O bending), and ν_1 (the symmetric P-O stretching). Only the absorptions of the ν_4 and ν_3 vibrations can be observed in the undistorted situation. The ν_2 and ν_1 vibrations are infrared inactive as the symmetry of the tetrahedral PO_4^{3-} is reduced [18, 19]. The FT-IR spectra of the Cd-FAP solids before and after dissolution are plotted together in Figure 2. The regular mode of the tetrahedral PO_4^{3-} ions in the prepared cadmium fluorapatite could be observed in the region around 949 cm^{-1} (ν_2), 1019 and 1100 cm^{-1} (ν_3), and 561 and 590 cm^{-1} (ν_4). The 712.60 cm^{-1} bands and the 3533~3537 cm^{-1} bands were assigned to the vibrational motion of OH^- ions and the stretching vibration of the bulk OH^- ions, respectively [4, 20]. The symmetric P-O stretching vibration (ν_1) was not visible. The bands at 871 cm^{-1}, which were related to HPO_4^{2-} ions presenting in cation-deficient apatite, had not been detected [4]. The bands at 3650~3680 cm^{-1} representing the P-OH groups [4] and the bands at 1455 cm^{-1} representing the CO_3^{2-} vibration [21] were also not observed in the FT-IR spectra.

As shown in Figure 3, the FE-SEM examination indicated that all the synthesized cadmium fluorapatite nanorods were the typical hexagonal crystals that elongated along the *c* axis (diameter <50 nm) and with or without pinacoids as terminations. No obvious morphological variation was found after dissolution for 7200 h.

3.2. Dissolution Mechanism. The solution Cd^{2+}, PO_4^{3-}, and F^- concentrations and pHs during the Cd-FAP dissolution at 25°C, 35°C, and 45°C and different pHs as a function of time are shown in Figures 4(a)–4(f).

The early dissolution of the cadmium fluorapatite in water was nearly stoichiometric and then nonstoichiometric. During the Cd-FAP dissolution at an initial pH of 2 and 25°C (Figure 4(a)), the solution pHs increased from 2.00 to 3.80 within 1 h and after that, varied between 3.72 and 3.95. The release rates of cadmium and phosphate increased quickly until the highest cadmium and phosphate concentrations appeared after 480 h and 1080 h, respectively. Thereafter, the total dissolution rate of Cd-FAP slowly declined while the solution Cd : P molar ratios increased continually from 1.55~1.67, which are near to the stoichiometric Cd : P molar ratio for Cd-FAP, to 3.18~3.22 (Figure 4(f)). Generally, the aqueous fluoride concentrations reached the highest value in 1 h and decreased rapidly from 1 h to 2160 h, and then, it increased slowly and attained a steady state after 5760 h. For the Cd-FAP dissolution at different temperatures, the solution pHs and aqueous Cd^{2+}, PO_4^{3-}, and F^- concentrations became constant after 5760 h indicating an achievement of a steady state between the solid and the solution (Figures 4(a)–4(c)).

Moreover, the initial solution pH (Figures 4(a), 4(d), and 4(e)) and the solution temperature (Figures 4(a)–4(c)) appeared to have an obvious influence on the dissolution and thereafter, the solution concentrations of Cd^{2+}, PO_4^{3-},

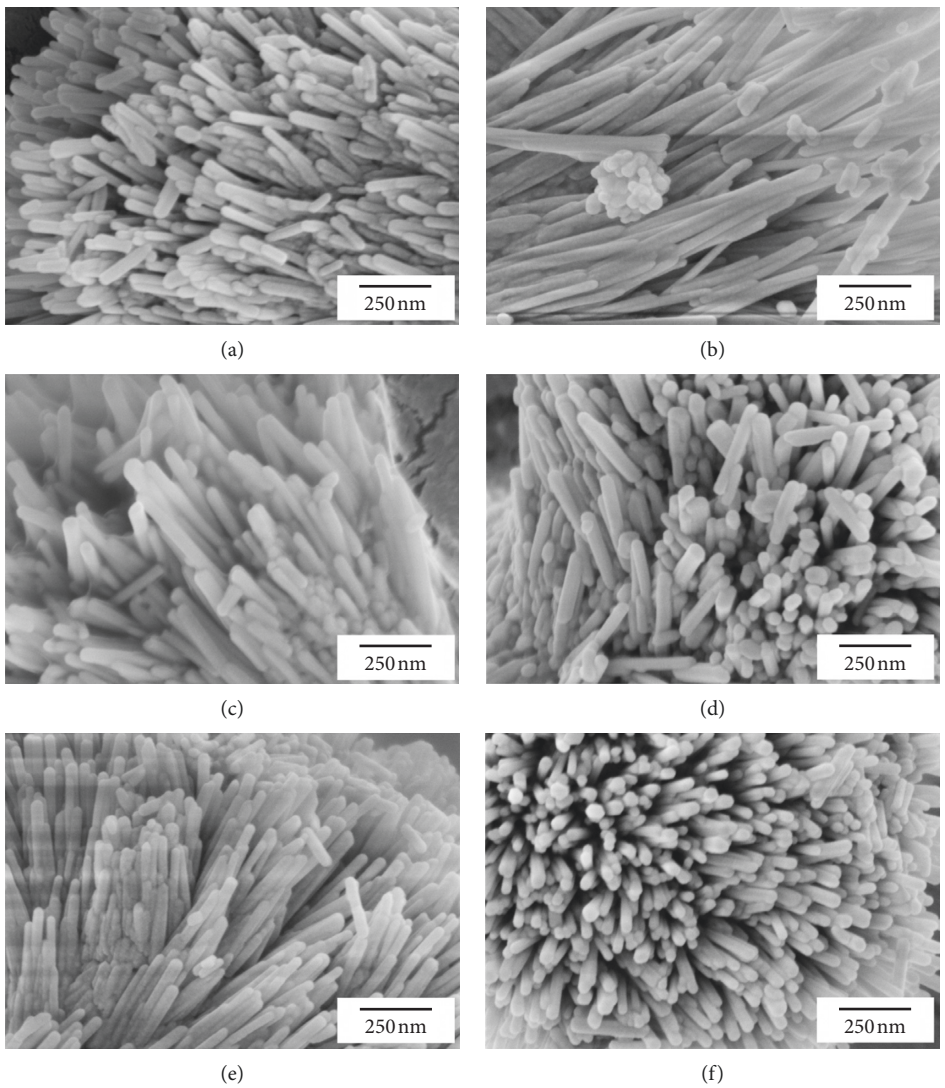

Figure 3: FE-SEM images of the synthetic cadmium fluorapatite [$Cd_5(PO_4)_3F$] before (a) and after (b)–(f) dissolution at 25–45°C for 7200 h. (a) Synthetic Cd-FAP; (b) 25°C and pH = 2; (c) 35°C and pH = 2; (d) 45°C and pH = 2; (e) 25°C and pH = 5.6; (f) 25°C and pH = 9.

and F^-. At the end of the dissolution, the solution concentrations of cadmium and phosphate at pH of 2.00 were higher than those at pH of 5.60 and 9.00, while the final pH and the solution concentration of fluoride at pH of 2.00 were lower than those at higher pHs. At the end of the dissolution, the solution concentrations of cadmium and fluoride at 35°C were a little lower than those at 25°C and 45°C, and the final pH and the solution concentration of phosphate at 35°C were a little higher than those at 25°C and 45°C (Figures 4(a)–4(c)). As a result, the aqueous Cd : P atomic ratios at 35°C were lower than those at 25°C and 45°C (Figure 4(f)). During the early dissolution (<120 h), the Cd^{2+} and PO_4^{3-} ions were released from Cd-FAP in the stoichiometric ratio with the dissolved Cd : P molar ratio being close to the stoichiometric ratio of 1.67 (Figure 4(f)). As the dissolution progressed, the solution Cd : P molar ratio rose and became larger than 1.67. This indicates that Cd^{2+} ions were preferentially released from the apatite structure in comparison with PO_4^{3-} ions during the Cd-FAP dissolution. The solution Cd : P molar ratios at 45°C were significantly higher than those at 25°C and 35°C, which indicated that the Cd-FAP solubility and dissolution processes were related to the dissolution temperature.

The transient peak values in the aqueous component concentrations during the apatite dissolution were also reported in some earlier works [13], which were probably due to the grain size distribution. The smaller the apatite grains, the greater the dissolution rate of apatite, and the larger the apatite solubility. Hence, the peak values may be a consequence of the fast dissolution of the smaller grains, followed by reprecipitation to larger grains, which resulted in the achievement of the asymptotic solubility [13].

The decrease in solution pH indicated that protons were consumed during the Cd-FAP dissolution, that is, the negatively charged O ions of surface PO_4^{3-} groups adsorbed protons from solution and transformed into HPO_4^{2-}, which accelerated the Cd-FAP dissolution. Additionally, the

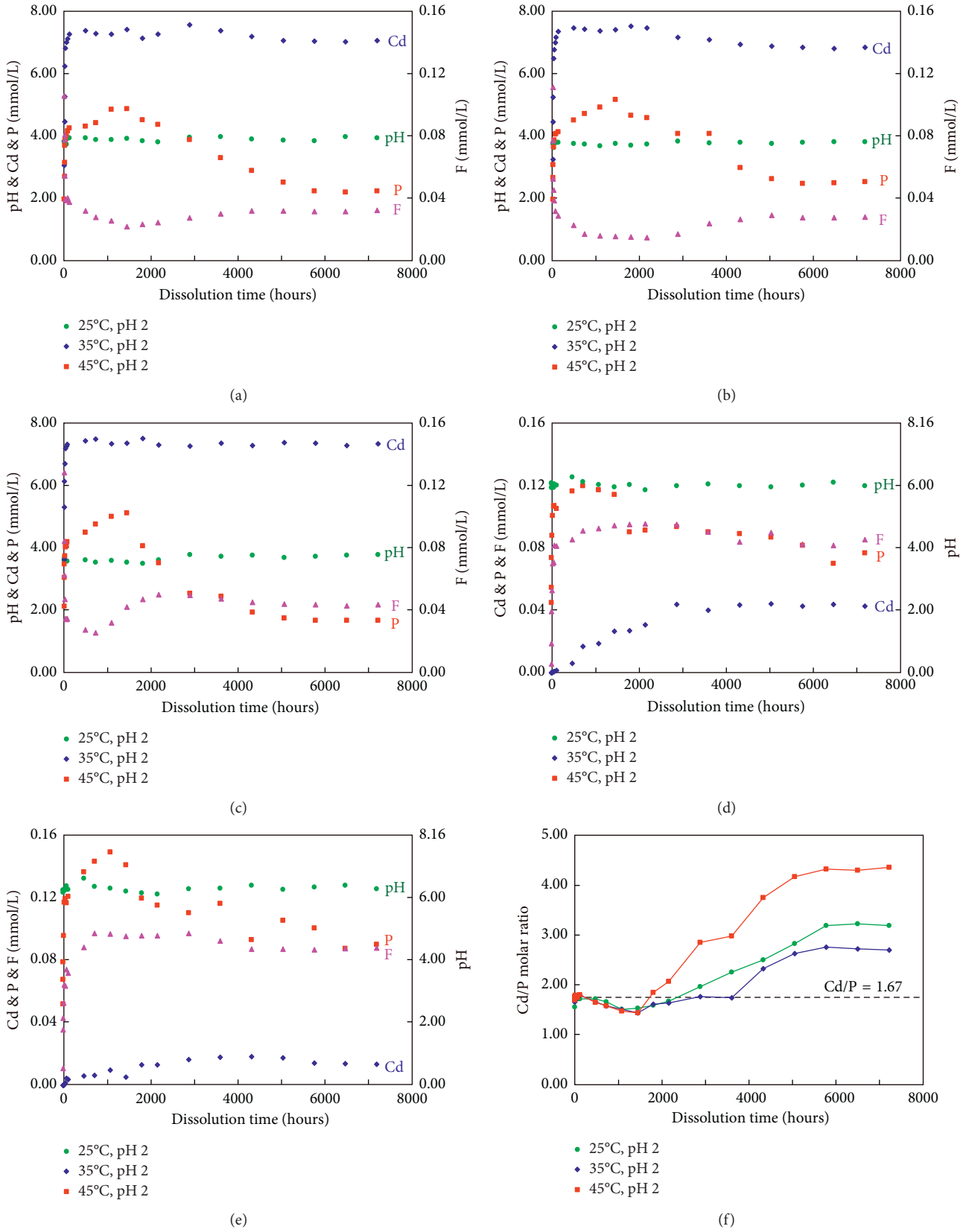

Figure 4: Aqueous evolution during the dissolution of the synthetic cadmium fluorapatite [$Cd_5(PO_4)_3F$] at 25–45°C for 7200 h. (a) 25°C and pH = 2; (b) 35°C and pH = 2; (c) 45°C and pH = 2; (d) 25°C and pH = 5.6; (e) 25°C and pH = 9; (f) Cd/P ratio.

stoichiometric ion exchange of $2H^+$ from solution for Cd^{2+} on the Cd-FAP surface and some other reactions also consumed protons [14, 21]. Besides, the dissolution mechanism of apatite is strongly dependent on the experimental condition such as temperature, solution composition, solid component, solid/solution ratio, and agitation [14]. Diverse models for the apatite dissolution have been proposed, but most of them take only some specific dissolution aspects into account and cannot describe the general dissolution mechanism of apatite [14].

Based on our experimental results and the data obtained for the apatite dissolution by different researchers, the cadmium fluorapatite (Cd-FAP) dissolution in the aqueous media is proposed to comprise the following simultaneous processes:

(i) Diffusion of protons from the aqueous solution to the Cd-FAP surface

(ii) H^+ adsorption onto the Cd-FAP surface coupled with protonation and chemical complexation/transformation on the Cd-FAP surface

(iii) Stoichiometric dissolution with Cd^{2+}, PO_4^{3-}, and F^- release from the Cd-FAP surface

(iv) Nonstoichiometric dissolution with Cd^{2+} and PO_4^{3-} release from the Cd-FAP surface and F^- adsorption backwards onto the Cd-FAP surface

(v) Nonstoichiometric dissolution with F^- release from the Cd-FAP surface and Cd^{2+} and PO_4^{3-} adsorption backwards onto the Cd-FAP surface

For the dissolution of the synthetic cadmium fluorapatite at 25°C and initial pH 2, in process (i) and process (ii), H^+ ions were adsorbed from the aqueous acidic solution to F^- ions as well as to the negative charged O ions of PO_4^{3-} groups on the Cd-FAP surface [22], which resulted in an increase in the solution pHs from 2.00 to 3.80 in 1 h of dissolution. In comparison with the negative charged O ions of PO_4^{3-} groups on the Cd-FAP surface, H^+ ions should be adsorbed preferentially to the F^- ions owing to their higher electronegativity [14]. Meanwhile, the surface PO_4^{3-} groups were transformed into HPO_4^{2-}, which would catalyze the apatite dissolution [23].

In process (iii), Cd^{2+}, PO_4^{3-}, and F^- ions were dissociated stoichiometrically from the Cd-FAP solid surface (reaction (1)); that is, the aqueous Cd^{2+}, PO_4^{3-}, and F^- concentrations increased simultaneously with a Cd : P : F molar ratio of 5 : 3 : 1 in the short early dissolution period.

Apatites are complex minerals, and when investigating their dissolution, several possible reactions must be considered [3]. The dissolution of Cd-FAP according to reaction (1) is strongly dependent on the solution pH and coupled with protonation and complexation reactions (2)–(4), which could result in an increase in the aqueous pHs for the Cd-FAP dissolution in the acidic solution or a decrease in the aqueous pHs for the dissolution in the alkali solution:

$$Cd_5(PO_4)_3F \leftrightharpoons 5Cd^{2+} + 3PO_4^{3-} + F^- \quad (1)$$

$$Cd^{2+} + nOH^- \leftrightharpoons Cd(OH)_n^{(n-2)-} \quad (n = 1\sim4) \quad (2)$$

$$PO_4^{3-} + nH^+ \leftrightharpoons H_nPO_4^{(3-n)-} \quad (n = 1\sim3) \quad (3)$$

$$H^+ + nF^- \leftrightharpoons HF_n^{(n-1)-} \quad (n = 1\sim2) \quad (4)$$

The speciation calculation using PHREEQC indicated that, for the Cd-FAP dissolution at 25°C and initial pH 2, the solution Cd species presented in the order of $Cd^{2+} > CdF^+$, $CdNO_3^+ > CdOH^+ > Cd_2OH^{3+} > Cd(OH)_2 > Cd(OH)_3^- > Cd(OH)_4^{2-}$; the solution phosphate species presented in the order of $H_2PO_4^- > H_3PO_4 > HPO_4^{2-} > PO_4^{3-}$; and the solution fluoride species presented in the order of $F^- > HF > CdF^+ \gg HF_2^-$.

In processes (iv) and (v), cadmium, phosphate, and fluoride ions were released from the Cd-FAP solid into solution nonstoichiometrically with the solution Cd : P molar ratios >1.67 and the solution Cd : F molar ratios >5.00, which might result in the formation of a surface layer with a component different from the bulk solid [14]. Some amount of cadmium, phosphate, and fluoride were adsorbed from the solution back onto the Cd-FAP surface after an initial portion of Cd-FAP had dissolved, the solution F concentrations had started to decrease gradually within 1 h of dissolution in the present experiment, the solution phosphate concentrations began to decrease gradually after 1440 h of dissolution, and the solution Cd concentrations began to decrease gradually after 2880 h of dissolution at 25°C and initial pH 2.

Fluorapatite dissolution might be started through a relatively fast and complete dissociation of F^- ions from the solid surface [14, 21]. In processes (iii)~(v), F^- ions were dissociated faster than cadmium and phosphate ions, and then the dissolved F^- ions were quickly adsorbed back to the Cd-FAP surface. As a result, the solution Cd : F ratio and P : F ratio became noticeably higher than the stoichiometric ratio of 5.00 and 3.00, respectively. The detachment of cadmium and phosphate ions followed the dissociation of F^- ions from the Cd-FAP surface. The F^- release was coupled to a quick hydrolysis of phosphate ions [21]. O ions of PO_4^{3-} groups cover 80~90% of the apatite surface [14]. $\equiv CdOH_2^+$ and $\equiv PO^-$ are thought to be the two distinct groups on the surface. According to the surface protonation model, the FAP surface protonation in the solution of pH 5~7 happened through the formation of $\equiv POH$ groups [24]. In the early dissolution of apatite (1–6 h), the solution Cd : P ratios (1.55~1.65) were a little smaller than its stoichiometric Cd : P ratio of 1.67, suggesting that PO_4^{3-} ions could be preferentially dissociated from the FAP surface in comparison to Cd^{2+} ions. The corners and edges of the apatite crystal were predominantly occupied by PO_4^{3-} ions, and the apatite dissolution could start through the complexation of H^+ ions from solution with these weakly bounded PO_4^{3-} groups on the solid surface [14].

Finally, the desorption-adsorption processes of cadmium, phosphate, and fluoride ions attained a steady state; that is, the solution cadmium, phosphate, and fluoride concentrations were constant for the Cd-FAP dissolution in the solution of pH 2 at 25°C from 5760 h to the end of experiment (7200 h).

3.3. Determination of Solubility. The aqueous Cd^{2+}, PO_4^{3-}, and F^- activities in the final equilibrated solution (5040 h, 5760 h, and 7200 h) were computed with the program PHREEQC to estimate the solubility product of the synthetic cadmium fluorapatite [$Cd_5(PO_4)_3F$]. The PHREEQC calculation also indicated that the final equilibrated solution was unsaturated with any possible secondary phases such as $Cd_3(PO_4)_2$, $Cd(OH)_2$, and monteponite (CdO).

The dissolution reaction of cadmium fluorapatite [$Cd_5(PO_4)_3F$] and the dissociation of Cd^{2+}, PO_4^{3-}, and F^- are expressed by the dissolution equation (1). Assuming unit activity of $Cd_5(PO_4)_3F$:

$$K_{sp} = \left\{Cd^{2+}\right\}^5 \left\{PO_4^{3-}\right\}^3 \{F^-\}, \tag{5}$$

where {} is the thermodynamic activities of the Cd^{2+}, PO_4^{3-}, and F^- species and K_{sp} is the solubility product of cadmium fluorapatite [$Cd_5(PO_4)_3F$] according to the dissolution equation (1).

The K_{sp} value under standard conditions (298.15 K and 0.101 MPa) is related to the standard free energy of reaction (ΔG_r^0) and can be described by

$$\Delta G_r^0 = -5.708 \log K_{sp}. \tag{6}$$

For Equation (1),

$$\begin{aligned}\Delta G_r^0 = {} & 5\Delta G_f^0\left[Cd^{2+}\right] + 3\Delta G_f^0\left[PO_4^{3-}\right] \\ & + \Delta G_f^0[F^-] - \Delta G_f^0\left[Cd_5(PO_4)_3F\right].\end{aligned} \tag{7}$$

By rearranging,

$$\begin{aligned}\Delta G_f^0\left[Cd_5(PO_4)_3F\right] = {} & 5\Delta G_f^0\left[Cd^{2+}\right] + 3\Delta G_f^0\left[PO_4^{3-}\right] \\ & + \Delta G_f^0[F^-] - \Delta G_r^0.\end{aligned} \tag{8}$$

Apatite group minerals are sparingly soluble. Table 1 gives the dissolution temperature, the initial solution pH, the final solution pH, and Cd, P, and F analyses together with the calculated solubility product of Cd-FAP. The aqueous activities of Cd^{2+}, PO_4^{3-}, and F^- were firstly computed with PHREEQC. The $\log K_{sp}$ value for $Cd_5(PO_4)_3F$ was then calculated after Equation (5). The average K_{sp} values were determined for $Cd_5(PO_4)_3F$ of $10^{-60.03}$ ($10^{-59.74}$~$10^{-60.46}$) at 25°C, $10^{-60.38}$ ($10^{-60.32}$~$10^{-60.48}$) at 35°C, and $10^{-60.45}$ ($10^{-60.33}$~$10^{-60.63}$) at 45°C, which were very close to the average K_{sp} values for $Ca_5(PO_4)_3F$ of $10^{-60.02}$ ($10^{-59.93}$~$10^{-60.14}$) at 25°C, $10^{-60.84}$ ($10^{-60.83}$~$10^{-60.85}$) at 25°C, and $10^{-61.13}$ ($10^{-61.02}$~$10^{-61.28}$) at 45°C (Tables 1 and 2). Based on the calculated K_{sp} values at the initial pH of 2 and 25°C, the Gibbs free energies of formation (ΔG_f^0) were estimated according to Equations (6)–(8) to be −4065.76 kJ/mol (−4064.11~−4068.23 kJ/mol) for $Cd_5(PO_4)_3F$ and −6445.51 kJ/mol (−6445.01~−6446.15 kJ/mol) for $Ca_5(PO_4)_3F$ (Table 1).

No solubility data for cadmium fluorapatite [Cd-FAP, $Cd_5(PO_4)_3F$] have been reported in literatures. The average K_{sp} value for $Cd_5(PO_4)_3F$ of $10^{-60.03}$ at 25°C was about 4.81 log units smaller than $10^{-55.22}$ for $Cd_5(PO_4)_3OH$ at 37°C [25] and 4.59 log units higher than $10^{-64.62}$ reported for $Cd_5(PO_4)_3OH$ at 25°C [26], while the K_{sp} values for $Ca_5(PO_4)_3F$ were reported to be $10^{-60.6}$ [27], 10^{-59} [28], 10^{-70} [12], and $10^{-55.71}$ [19]. This significant difference in the solubility product is thought to be related to the difference in the dissolution conditions and the hydroxyapatite materials used in the different experiments [3].

3.4. Determination of Thermodynamic Data. The solubility products (K_{sp}) for Cd-FAP and Ca-FAP can also be estimated using Equations (9)–(11) [25]:

$$-\log K_{sp} = \frac{A}{T} + B + CT. \tag{9}$$

For Cd-FAP,

$$-\log K_{sp} = -\frac{40857.3723}{T} + 319.3293 - 0.4100T. \tag{10}$$

For Ca-FAP,

$$-\log K_{sp} = -\frac{77482.5843}{T} + 547.2256 - 0.7624T. \tag{11}$$

The thermodynamic quantities ΔG^0, ΔH^0, ΔS^0, and ΔC_p^0 for the Cd-FAP and Ca-FAP dissolution at an initial pH of 2 are estimated after Equations (12)–(15) [25] and given in Table 2:

$$\Delta G^0 = 2.3026R\left(A + BT + CT^2\right), \tag{12}$$

$$\Delta H^0 = 2.3026R\left(A - CT^2\right), \tag{13}$$

$$\Delta S^0 = -2.3026R\,(B + 2CT), \tag{14}$$

$$\Delta C_p^0 = -2.3026R\,(CT), \tag{15}$$

where A, B, and C are the empirical constants of Equation (9).

The negative values of ΔH^0 indicated that the Cd-FAP and Ca-FAP dissolution in the aqueous solution was an exothermic reaction, and their solubilities declined with the temperature rising. The larger negative value of ΔS^0 for the Cd-FAP dissolution showed that the order produced by the cadmium cations in the aqueous solution was a little higher than that by calcium cations [25], which was related to the ion size difference between Ca^{2+} (0.99 Å) and Cd^{2+} (0.97 Å). Generally, the smaller Cd^{2+} ions with a high charge can result in a lower entropy in aqueous solution, and consequently, Cd-FAP is less soluble than Ca-HAP. But the very similar ion sizes of Cd^{2+} and Ca^{2+} resulted in a close solubility product for Cd-FAP and Ca-HAP under the experimental conditions. The values of ΔG^0, ΔH^0, and ΔS^0 for the Cd-FAP and Ca-HAP dissolution increased with the increasing temperature and indicated that their dissolution was an energy-consuming process [25].

4. Conclusions

The synthetic cadmium fluorapatite [$Cd_5(PO_4)_3F$] was the typical hexagonal columnar nanorod crystals (diameter <50 nm) with or without a pinacoid as a termination, which elongated along the *c* axis with the lattice cell parameters of

Table 1: Analytical data and solubility product of cadmium fluorapatite [$Cd_5(PO_4)_3F$].

Temperature (°C)	Initial pH	Reaction time (hour)	Analytical data				$\log K_{sp}$	ΔG_f^0 (kJ/mol)
			pH	Cd (mmol/L)	P (mmol/L)	F (mmol/L)		
25	2.00	5040	3.83	7.0385	2.2094	0.0311	−60.46	−4068.23
		5760	3.95	7.0154	2.1788	0.0312	−59.74	−4064.11
		7200	3.92	7.0474	2.2127	0.0319	−59.89	−4064.96
35	2.00	5040	3.78	6.8019	2.4679	0.0276	−60.48	—
		5760	3.80	6.7681	2.4834	0.0275	−60.35	—
		7200	3.80	6.8037	2.5215	0.0278	−60.32	—
45	2.00	5040	3.74	7.3463	1.6982	0.0437	−60.63	—
		5760	3.78	7.2840	1.6924	0.0432	−60.40	—
		7200	3.79	7.3356	1.6821	0.0439	−60.33	—
25	5.60	5040	6.01	0.0426	0.0814	0.0822	−61.20	−4072.43
		5760	6.10	0.0438	0.0698	0.0814	−60.82	−4070.27
		7200	5.98	0.0427	0.0768	0.0853	−61.43	−4073.74
25	9.00	5040	6.35	0.0143	0.1006	0.0869	−61.31	−4073.05
		5760	6.41	0.0139	0.0877	0.0876	−61.21	−4072.48
		7200	6.29	0.0137	0.0904	0.0882	−61.87	−4076.25

Table 2: Thermodynamic data of Cd-FAP than Ca-FAP in the aqueous acidic media (an initial pH of 2).

FAP	Temperature (°C)	Average $\log K_{sp}$	ΔG^0 (J/K·mol)	ΔH^0 (J/mol)	ΔS^0 (J/K·mol)	ΔC_p^0 (J/K·mol)
Ca-FAP	25	−60.02	342473.29	−187235.69	−1777.55	4349.85
	35	−60.84	358789.08	−98779.03	−1485.61	4495.82
	45	−61.13	372185.51	−7403.00	−1193.67	4641.79
Cd-FAP	25	−60.03	342515.78	−85088.80	−1434.91	2339.50
	35	−60.38	356079.86	−37513.71	−1277.90	2418.01
	45	−60.45	368073.80	11631.51	−1120.89	2496.51

$a = 9.3284$ and $c = 6.6378$. The essential vibrational modes of PO_4^{3-} tetrahedra appeared at 949 cm^{-1} (ν_2), 1019 and 1100 cm^{-1} (ν_3), and 561 and 590 cm^{-1} (ν_4).

For the Cd-FAP dissolution at an initial pH of 2 and 25°C, the dissociation rates of fluoride, phosphate, and cadmium increased quickly until their highest solution concentrations were attained after dissolution for <1 h, 1440 h, and 2880 h, respectively. After that, the Cd-FAP dissolution decreased slowly while the solution Cd/P molar ratios increased steadily from 1.65~1.67 to 3.18~3.22. The solution pH increased from 2.00 to 3.80 within 1 h and then varied between 3.72 and 3.95.

The average K_{sp} values were determined for $Cd_5(PO_4)_3F$ of $10^{-60.03}$ at 25°C, $10^{-60.38}$ at 35°C, and $10^{-60.45}$ at 45°C. Based on K_{sp} at an initial pH of 2 and 25°C, the Gibbs free energy of formation (ΔG_f^0) was calculated to be −4065.76 kJ/mol. The thermodynamic quantities, ΔG^0, ΔH^0, ΔS^0, and ΔC_p^0, for the Cd-FAP dissolution at an initial pH of 2 and 25°C were determined to be 342515.78 J/K·mol, −85088.80 J/mol, −1434.91 J/K·mol, and 2339.50 J/K·mol, respectively.

Data Availability

The powder XRD data in XML format, the FT-IR data in XLSX format, and all solution analytical data in XLSX format used to support the findings of this study are available from the corresponding author upon request.

Conflicts of Interest

The authors declare that there are no conflicts of interest regarding the publication of this paper.

Acknowledgments

This work was financially supported by the National Natural Science Foundation of China (41763012, 41263009, and 21707024), the Guangxi Science and Technology Planning Project (GuiKe-AD18126018), the Special Fund for Guangxi Distinguished Experts, and the Provincial Natural Science Foundation of Guangxi (2014GXNSFBA118054).

References

[1] M. Masaoka, A. Kyono, T. Hatta, and M. Kimata, "Single crystal growth of $Pb_5(P_xAs_{1-x}O_4)_3Cl$ solid solution with apatite type structure," *Journal of Crystal Growth*, vol. 292, no. 1, pp. 129–135, 2006.

[2] M. C. F. Magalhães and P. A. Williams, "Chapter 18–apatite group minerals: solubility and environmental remediation," in *Thermodynamics Solubility and Environmental Issues*, pp. 327–340, Elsevier BV, New York City, NY, USA, 2007.

[3] Å. Bengtsson, A. Shchukarev, P. Persson, and S. Sjöberg, "A solubility and surface complexation study of a non-stoichiometric hydroxyapatite," *Geochimica et Cosmochimica Acta*, vol. 73, no. 2, pp. 257–267, 2009.

[4] A. Yasukawa, M. Higashijima, K. Kandori, and T. Ishikawa, "Preparation and characterization of cadmium–calcium

hydroxyapatite solid solution particles," *Colloids and Surfaces A Physicochemical and Engineering Aspects*, vol. 268, no. 1–3, pp. 111–117, 2005.

[5] M. S. Rosmi, S. Azhari, and R. Ahmad, "Adsorption of cadmium from aqueous solution by biomass: comparison of solid pineapple waste, sugarcane bagasse and activated carbon," *Advanced Materials Research*, vol. 832, no. 2014, pp. 810–815, 2013.

[6] M. Mahmood-Ul-Hassan, V. Suthar, E. Rafique, R. Ahmad, and M. Yasin, "Kinetics of cadmium, chromium, and lead sorption onto chemically modified sugarcane bagasse and wheat straw," *Environmental Monitoring and Assessment*, vol. 187, no. 7, pp. 1–11, 2015.

[7] N. Harouiya, C. Chaïrat, S. J. Köhler, R. Gout, and E. H. Oelkers, "The dissolution kinetics and apparent solubility of natural apatite in closed reactors at temperatures from 5 to 50°C and pH from 1 to 6," *Chemical Geology*, vol. 244, no. 3-4, pp. 554–568, 2007.

[8] R. Zhu, R. Yu, J. Yao, D. Mao, C. Xing, and D. Wang, "Removal of Cd^{2+} from aqueous solutions by hydroxyapatite," *Catalysis Today*, vol. 139, no. 1-2, pp. 94–99, 2008.

[9] F. Fernane, M. O. Mecherri, P. Sharrock, M. Hadioui, H. Lounici, and M. Fedoroff, "Sorption of cadmium and copper ions on natural and synthetic hydroxylapatite particles," *Materials Characterization*, vol. 59, no. 5, pp. 554–559, 2008.

[10] S. B. Chen, Y. B. Ma, L. Chen, and K. Xian, "Adsorption of aqueous Cd^{2+}, Pb^{2+}, Cu^{2+} ions by nano-hydroxyapatite: single- and multi-metal competitive adsorption study," *Geochemical Journal*, vol. 44, no. 3, pp. 233–239, 2010.

[11] Y. Zhu, Z. Zhu, X. Zhao, Y. Liang, L. Dai, and Y. Huang, "Characterization, dissolution and solubility of cadmium–calcium hydroxyapatite solid solutions at 25°C," *Chemical Geology*, vol. 423, pp. 34–48, 2016.

[12] E. Valsami-Jones, K. W. Ragnarsdottir, A. Putnis, D. Bosbach, A. J. Kemp, and G. Cressey, "The dissolution of apatite in the presence of aqueous metal cations at pH 2–7," *Chemical Geology*, vol. 151, no. 1–4, pp. 215–233, 1998.

[13] M. T. Fulmer, I. C. Ison, C. R. Hankermayer, B. R. Constantz, and J. Ross, "Measurements of the solubilities and dissolution rates of several hydroxyapatites," *Biomaterials*, vol. 23, no. 3, pp. 751–755, 2002.

[14] S. V. Dorozhkin, "A review on the dissolution models of calcium apatites," *Progress in Crystal Growth and Characterization of Materials*, vol. 44, no. 1, pp. 45–61, 2002.

[15] W. J. Tseng, C. C. Lin, P. W. Shen, and P. Shen, "Directional/acidic dissolution kinetics of (OH,F,Cl)-bearing apatite," *Journal of Biomedical Materials Research Part A*, vol. 76, no. 4, pp. 753–764, 2006.

[16] K. Skartsila and N. Spanos, "Surface characterization of hydroxyapatite: potentiometric titrations coupled with solubility measurements," *Journal of Colloid & Interface Science*, vol. 308, no. 2, pp. 405–412, 2007.

[17] D. L. Parkhurst and C. A. J. Appelo, "Description of input and examples for PHREEQC version 3—a computer program for speciation, batch-reaction, one-dimensional transport, and inverse geochemical calculations," in *Techniques and Methods, Book 6, Chapter A43*, pp. 1–497, U.S. Geological Survey, Reston, VA, United States, 2013.

[18] V. M. Bhatnagar, "X-Ray and infrared studies of lead apatites," *Canadian Journal of Chemistry*, vol. 49, no. 4, pp. 662-663, 1971.

[19] Y. Zhu, X. Zhang, Y. Chen et al., "A comparative study on the dissolution and solubility of hydroxylapatite and fluorapatite at 25°C and 45°C," *Chemical Geology*, vol. 268, no. 1-2, pp. 89–96, 2009.

[20] A. Yasukawa, T. Yokoyama, and T. Ishikawa, "Preparation of cadmium hydroxyapatite particles using acetamide," *Materials Research Bulletin*, vol. 36, no. 3-4, pp. 775–786, 2001.

[21] G. R. Qian, H.-M. Bai, F.-C. Sun, J.-Z. Zhou, W.-M. Sun, and X. Xu, "Preparation and stability of calcium cadmium hydroxyapatite," *Journal of Inorganic Materials*, vol. 23, no. 5, pp. 1016–1020, 2008.

[22] J. Christoffersen and M. R. Christoffersen, "Kinetics of dissolution of calcium hydroxyapatite: V. The acidity constant for the hydrogen phosphate surface complex," *Journal of Crystal Growth*, vol. 57, no. 1, pp. 21–26, 1982.

[23] J. Christoffersen, M. R. Christoffersen, and T. Johansen, "Some new aspects of surface nucleation applied to the growth and dissolution of fluorapatite and hydroxyapatite," *Journal of Crystal Growth*, vol. 163, no. 3, pp. 304–310, 1996.

[24] L. Wu, W. Forsling, and A. Holmgren, "Surface complexation of calcium minerals in aqueous solution," *Journal of Colloid and Interface Science*, vol. 147, no. 2, pp. 211–218, 2000.

[25] P. P. Mahapatra, H. Mishra, and N. S. Chickerur, "Solubility and thermodynamic data of cadmium hydroxyapatite in aqueous media," *Thermochimica Acta*, vol. 54, no. 1, pp. 1–8, 1982.

[26] Y. Zhu, Z. Zhu, X. Zhao, Y. Liang, L. Dai, and Y. Huang, "Characterization, dissolution and solubility of synthetic cadmium hydroxylapatite $[Cd_5(PO_4)_3OH]$ at 25–45°C," *Geochemical Transactions*, vol. 16, no. 1, pp. 1–11, 2015.

[27] F. C. Driessens, "Mineral aspects of dentistry," *Monographs in Oral Science*, vol. 10, pp. 1–215, 1982.

[28] W. Stumm and J. J. Morgan, *Aquatic Chemistry, Chemical Equilibria and Rates in Natural Waters*, John Wiley & Sons, New York, NY, USA, 1996.